N78-30454

FEATURE DISCRIMINATION/IDENTIFICATION BASED UPON SAR RETURN VARIATIONS

WILLIAM A. RASCO, SR. AND ROY PIETSCH
AEROSPACE TECHNOLOGY DIVISION
APPLIED RESEARCH LABORATORIES
THE UNIVERSITY OF TEXAS AT AUSTIN
P. O. BOX 8029, AUSTIN, TEXAS 78712

SUMMARY

A study of the statistics of the look-to-look variations in the returns recorded in-flight by a digital, realtime SAR system is being conducted for the Avionics Laboratory, Radar Branch, WPAFB, under USAF Contract F33615-77-C 1169. The study objectives include the determination of whether these variations demonstrate class-unique information content adequate to allow the use of some measure of that variance in discriminating between or identifying any or all of various classes of objects and features mapped by the SAR system. This paper briefly discusses the data, their source, the techniques employed in sampling, and some measures under study and presents a demonstration of the positive results thus far obtained toward meeting the objective defined above. The determination that the variations in the look-to-look returns from different classes do carry information content unique to the classes is illustrated by means of a model based on four variants derived from the four look in-flight SAR data under study. The model was limited to four classes of returns: mowed grass on a athletic field, rough unmowed grass and weeds on a large vacant field, young fruit trees in a large orchard, and metal mobile homes and storage buildings in a large mobile home park in Reedley, California. A data population in excess of 1000 returns, distributed between the four classes, was selected. These returns represent over 250 individual pixels from the four classes. The multivariant discriminant model operated on the set of returns for each pixel and assigned that pixel to one of the four classes, based on the target variants and the probability distribution function of the four variants for each class. The model, the variants used, and the test results are presented.

1.0 OBJECTIVES AND GENERAL APPROACH

1.1 OBJECTIVES

The overall objective of the study is to analyze the look-to-look variations of the multilook SAR returns from selected objects and features to determine whether some measure of that variance can be used in discriminating between or identifying any or all of the features and objects analyzed.

1.2 GENERAL APPROACH

The general approach is to analyze the variations of the returns from each of a number of sets of actual multilook returns representing statistically significant samples of selected classes and subclasses of known objects and features.

These sample sets are comprised of the radar returns associated with single pixels identifiable with known objects and features. The single pixels are selected interior to gross features, scene segments, or objects (i.e., individual trees within an orchard or grove, individual structures within a group or within a cluster of structures or trees, etc.)

Initial designation of classes and subclasses to be sampled was based on a requirement to obtain a realistic spread of variations and power levels. Additional classes and subclasses have been added as the study has progressed. All selections are based on ground truth information to minimize the number of "wild points" which may occur.

2.0 DATA SOURCE AND THE SELECTION PROCESS

2.1 SOURCE OF DATA

The SAR returns used in the study are obtained from digital data recorded in flight on wideband magnetic tapes during the recently concluded, USAF-conducted, 72-flight experimental flight test series with the in-flight, real-time data processing FLAMR (Forward Looking Airborne Multimode Radar) system . This system operated in the 16 to 16.5 GHz band .

Approximately 450 wideband, 30.5 x 2.5 cm (14 x 1 in.), 14-track magnetic tapes were recorded during the flight test program. These tapes and associated data and equipment are now located in the SAR Data Bank at the Applied Research Laboratories, The University of Texas at Austin (ARL:UT). The Data Bank is maintained for purposes of supplying SAR data to qualified, Air Force-

approved members of the technical and scientific community. The Data Base is
supported by the Air Force through USAF Contract F33615-77-C-1169 with ARL:UT.

2.2 THE SELECTION PROCESS

The flight data to be examined are identified by review of the documentation,
the available ground truth data, and photographs of the imagery associated
with various flights.

The next step is to replay the appropriate wideband tape corresponding
to the selected leg of a flight. This replay is accomplished by means of the
wideband tape drive shown on the right in the photograph in Fig. 1. The
recorded imagery is reviewed on the Monitor Display in 16 gray level format.
The DBS imagery used in the study is shown on the display in 360 vertical
lines comprised of 384 range bins each.
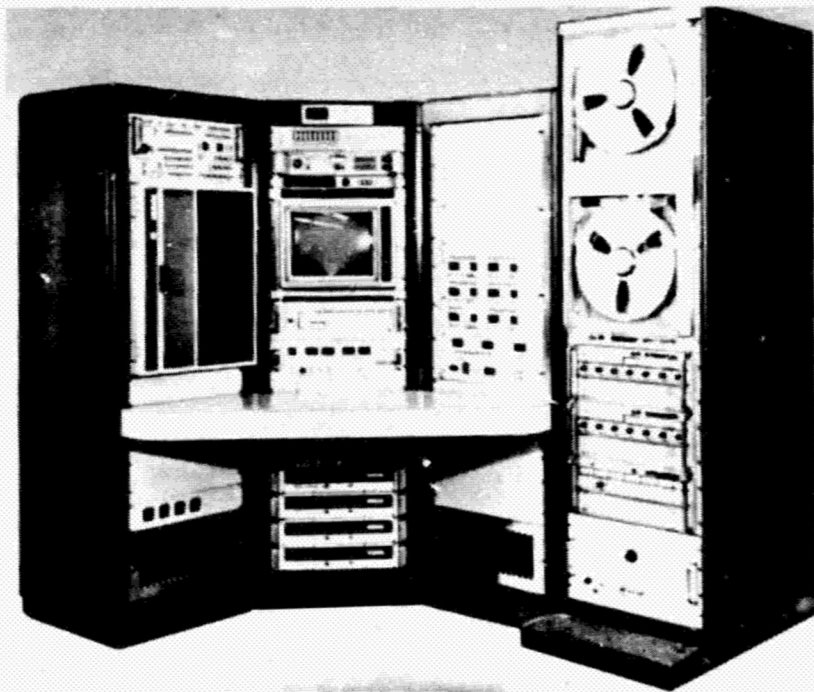
FIGURE 1.   SAR DATA BANK FLIGHT DATA RETRIEVAL EQUIPMENT

When the desired map is painted on the display, the image is then "frozen"
and the tape drive halted. The desired objects or features to be sampled are
then located on the display. To locate the brightest pixel in the case of
small discrete objects, the set of gray scale emphasis or deletion switches
below the monitor is used. To obtain the azimuth line and range bin
numbers of a selected pixel, the manual controls below the display are

used to position a local cursor over the pixel. The desired coordinates are then read directly from the cursor controls.

After all desired sample pixels on the scan have been identified and coordinates noted, a CCT (Computer-Compatible Tape) is placed on the small tape drive visible at the left in Fig. 1. The data select/dump controls on the panel to the right of the display are then set to dump the desired data. The practice thus far in the study has been to dump the full scan of FM data (Filter Magnitudes recorded in flight at the output of the Doppler Processor) and a file of the associated RIOT data (Radar Input-Output data recorded from the radar-computer I/O bus). The flight data are in computer-compatible format and are processed on a general purpose computer.

The FM data are next reformatted and five arrays of FM data, similar to those appearing in Fig. 2, are printed for each selected pixel for use in checking

FIGURE 2.   FM PRINTOUT FOR 35-PIXEL SECTIONS OF THE FOUR
SINGLE-FREQUENCY AND THE COMPOSITE 4:1 MAPS

and finalizing the selection and coordinates for the sample pixels. The FM values appearing in Map 1234, the composite 4:1 overlaid map, are examined to verify that the selected coordinates of the center point of the printout array represent, for the case of a small discrete, the brightest return from

the discrete. If an immediately adjacent pixel has a higher FM value, then the coordinates are changed to the coordinates of the brighter pixel. Thus far in the study, no further effort to correct for range/Doppler straddling has been made. After the coordinates are finalized, they are used with computer programs and the two data tapes, FM and RIOT, to combine the returns data and other required information on a punched card for each sample pixel. The punched cards are then used as the data base for analysis.

2.3 THE TEST CASE

A photograph of the imagery from which the sample sets treated in this paper were obtained is shown in Fig. 4. This imagery is one of the DBS scans made during a mapping flight in the San Joaquin Valley area of California near the town of Reedley. This scan was chosen for sampling because of the diversity of terrain, vegetation, and cultural features and the large Data Bank stock of photographs of various portions of the town and nearby countryside. Figure 3(A) is a photograph of a mowed grass athletic field located just above and to the right of the two bridges visible in the upper left corner of Fig. 4. The samples comprising sample class 201 were obtained from this location on the imagery.

Figure 3(B) is a photograph of a large vacant field covered with rough grass and weeds and located to the right of the group of bright returns from the buildings located just left of center at the extreme top edge of Fig. 4. The samples from this field comprise class 202. It was anticipated that there would be substantial overlap between the variants for classes 201 and 202, and the two similar features were selected for this reason.

Class 102 is comprised of fruit trees from the orchard shown in Fig. 3(C). This orchard is the large triangular area located just above the river in the lower right quadrant of Fig. 4.

Class 9000 was selected from the rectangular cluster of bright returns just below the sharp bend in the river in the lower right corner of Fig. 4. These returns are from a large mobile home park, visible in Fig. 3(D).
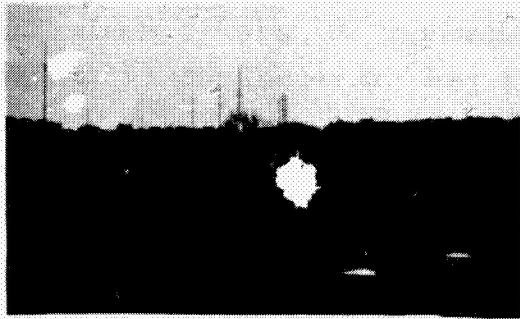
A. CLASS 201

B. CLASS 202

C. CLASS 102

D. CLASS 9000

FIGURE 3.   PHOTOGRAPHS OF TEST SAMPLE SOURCE AREAS

3.0   THE DATA

3.1   FORMATION AND COMPOSITION OF THE FIVE MAPS

Since the I and Q data available   the Data Bank have not yet been studied, only the FM data will be discussed here. As shown in the printout of FM data illustrated in Fig. 2, there are five arrays of 5 x 7 FM values each, a total of 35 pixels. Each array carries a MAP number and an FRQ value code to the right of the array, with the exception of the array at the bottom of the figure. The column of numbers on the left edge of the picture contains the range bin coordinate for the associated row of pixels, and the map line numbers above the top array denote the azimuth coordinate for the associated column of pixels. The arrays for maps 1, 2, 3, and 4 are obtained from the four complete 1:1 overlay ratio, single frequency maps formed in the process of producing the 4:1 overlay map from which the bottom array is obtained.

FIGURE 4

SAR MAP OF REEDLEY, CALIFORNIA,
DBS 4:1 OVERLAY
(SAMPLE AREA FOR TEST CASE)

Note that each pixel with a given range bin and azimuth line set of
coordinates is represented in all five arrays.

```
ARRAY No.   |←─Array-1 ─→| |←─Array-5 ─→| |←─Array-9 ─→|
LINE No.    1 2 3 4 5 6 7 8 1 2 3 4 5 6 7 8 1 2 3 4 5 6 7 8 - - - - - - - - -
MAP-1
FREQ.=f₀    | | | | | | | | | | | | | | | | | | | | | | | |


ARRAY No.     |←─Array-2 ─→| |←─Array-6 ─→| |←─Array-10 ─→|
LINE No.      1 2 3 4 5 6 7 8 1 2 3 4 5 6 7 8 1 2 3 4 5 6 7 8 - - - - - - -
MAP-2
FREQ.=f₁      | | | | | | | | | | | | | | | | | | | | | | | |


ARRAY No.       |←─Array-3 ─→| |←─Array-7 ─→| |←─Array-11 ─→|
LINE No.        1 2 3 4 5 6 7 8 1 2 3 4 5 6 7 8 1 2 3 4 5 6 7 8 - - - -
MAP-3
FREQ.=f₂        | | | | | | | | | | | | | | | | | | | | | | | | !


ARRAY No.         |  Array-4 ─→| |←─Array-8 ─→| |←─Array-12 ─→|
LINE No.          1 2 3 4 5 6 7 8 1 2 3 4 5 6 7 8 1 2 3 4 5 6 7 8 - -
MAP-4
FREQ.=f₃          | | | | | | | | | | | | | | | | | | | | | | | |


4:1 Overlaid
LINE No.          1 2 3 4 5 6 7 8 9 10 12  14   16   18   20   22   24 - -
MAP-1234          | | | | | | | | | | | | | | | | | | | | | | | |
```

The FRQ value given for each of the 1:1 overlay maps represents the trans-
mitter frequency used in the formation of that map for this particular scan.
This frequency varies from flight to flight and from scan to scan, but its
cycle of occurrence does not vary. The cycle sequence is in order of descend-
ing frequency (i.e., 16.4, 16.3, 16.2, 16.1, or any combination such as 16.3,
16.2, 16.1, 16.4, and so on). When the "frequency hop" mode was employed, as
it often was, the transmitter frequency changed for each 8-azimuth-line
array formed.

III-1-8

Note that each pixel with a given range bin and azimuth line set of
coordinates is represented in all five arrays.

```
ARRAY No.   |←─Array-1 ─→| |←─Array-5 ─→| |←─Array-9 ─→|
LINE No.    1 2 3 4 5 6 7 8 1 2 3 4 5 6 7 8 1 2 3 4 5 6 7 8 - - - - - - - - -
MAP-1
FREQ.=f₀    | | | | | | | | | | | | | | | | | | | | | | | |


ARRAY No.     |←─Array-2 ─→| |←─Array-6 ─→| |←─Array-10 ─→|
LINE No.      1 2 3 4 5 6 7 8 1 2 3 4 5 6 7 8 1 2 3 4 5 6 7 8 - - - - - - -
MAP-2
FREQ.=f₁      | | | | | | | | | | | | | | | | | | | | | | | |


ARRAY No.       |←─Array-3 ─→| |←─Array-7 ─→| |←─Array-11 ─→|
LINE No.        1 2 3 4 5 6 7 8 1 2 3 4 5 6 7 8 1 2 3 4 5 6 7 8 - - - -
MAP-3
FREQ.=f₂        | | | | | | | | | | | | | | | | | | | | | | | | !


ARRAY No.         |  Array-4 ─→| |←─Array-8 ─→| |←─Array-12 ─→|
LINE No.          1 2 3 4 5 6 7 8 1 2 3 4 5 6 7 8 1 2 3 4 5 6 7 8 - -
MAP-4
FREQ.=f₃          | | | | | | | | | | | | | | | | | | | | | | | |


4:1 Overlaid
LINE No.          1 2 3 4 5 6 7 8 9 10 12  14   16   18   20   22   24 - -
MAP-1234          | | | | | | | | | | | | | | | | | | | | | | | |

                  x x x x x x x x x x x x x x x x x x x x x x x x
PIXEL No.         1 2 3 4 5 6 7 8 9 10 12  14   16   18   20   22   24
 Return
time sequence     f₀ f₁ f₂ f₃ f₀ f₁ f₂ f₃ f₀ f₁ f₂ f₃

                  f₁ f₂ f₃ f₀ f₁ f₂ f₃ f₀ f₁ f₂ f₃ f₀

                  f₂ f₃ f₀ f₁ f₂ f₃ f₀ f₁ f₂ f₃ f₀ f₁

                  f₃ f₀ f₁ f₂ f₃ f₄ f₁ f₂ f₃ f₀ f₁ f₂
```
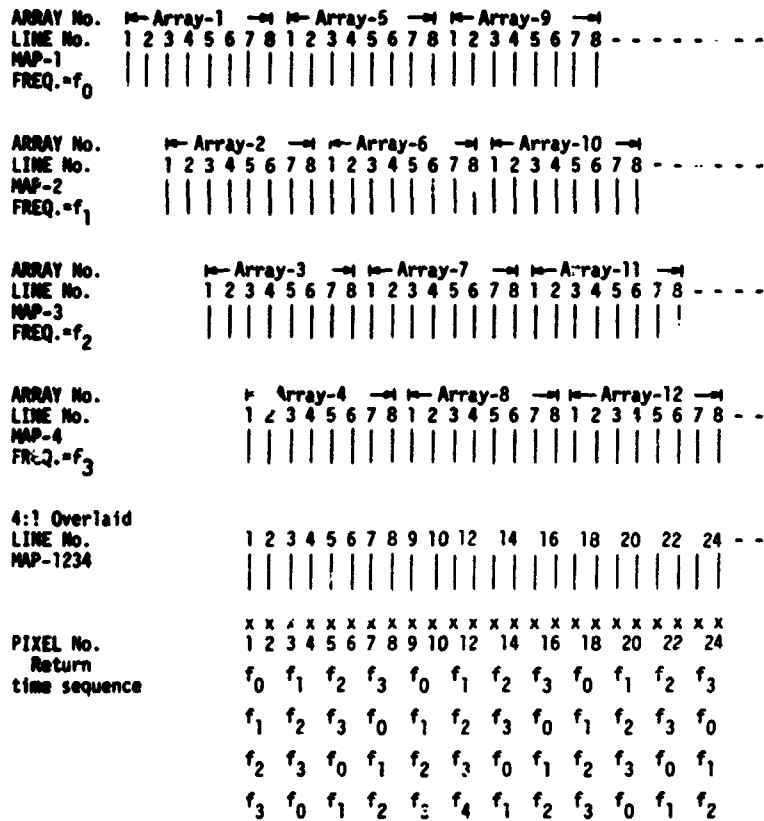
FIGURE 5 - FORMATION OF MAP OVERLAY LINES WITH
ASSOCIATED FREQUENCY SEQUENCE OF RETURNS

The FRQ value given for each of the 1:1 overlay maps represents the trans-
mitter frequency used in the formation of that map for this particular scan.
This frequency varies from flight to flight and from scan to scan, but its
cycle of occurrence does not vary. The cycle sequence is in order of descend-
ing frequency (i.e., 16.4, 16.3, 16.2, 16.1, or any combination such as 16.3,
16.2, 16.1, 16.4, and so on). When the "frequency hop" mode was employed, as
it often was, the transmitter frequency changed for each 8-azimuth-line
array formed.

III-1-8

The method of overlay employed in forming the separate 1:1 maps and the composite 4:1 overlay map is illustrated in Fig. 5. The key datum which the authors wish to convey here is the association of a particular frequency sequence with each pair of azimuth lines in the composite 4:1 overlay map, which is formed by averaging together the appropriate pixels from the four 1:1 maps, 1, 2, 3, and 4. Note that three 8-line arrays are presented for each of the four 1:1 maps and that each array bears an array number, representing the order in which the arrays are formed by the system. Array No. 1 is formed first, then array No. 2 is formed but with an azimuth displacement of two azimuth lines to the right. Next come arrays No. 3 and No. 4, respectively, each with an additional 2-line displacement relative to the preceding array.

After the first four arrays are formed, note that there are only two azimuth lines of the 4:1 map that can be formed by averaging together the corresponding lines of the four 1:1 maps. Thus, lines 7,8 of array No. 1, lines 5,6 of array No. 2, lines 3,4 of array No. 3, and lines 1,2 of array No. 4 correspond in azimuth and, averaged together, form lines 1,2 of the 4:1 map.

The row of x's below the 4:1 map denotes pixels on each map azimuth line. The column of f's below each pair of x's denotes the time order in which each return frequency will be received by the SAR. For pixels 1 and 2, the first transmitter frequency illuminating these points was f_0, then, in order f_1, f_2, and f_3. For the next pair of pixels the first frequency will be f_1, from lines 7 and 8 of array No. 2. The rest of the sequence is f_2 from lines 5,6 of array No. 3, f_3 from lines 3,4 of array No. 4, and finally, f_0 from array No. 5. These sequences continue to cycle throughout the map. This varying frequency sequencing has been found to be quite important in the study of variants and the study of its effects is continuing.

3.2 SCINTILLATION

Four enlarged 1:1 map strips of the mobile home park and adjoining fields shown previously in Figs. 3(D) and 4 are presented in Fig. 6. Note the map-to-map variations in the pattern of returns from the structures in the park and the surrounding fields. Gray level 8 was emphasized in these pictures and the higher gray shades were deleted to better illustrate the variations.

FIGURE 6   MOBILE HOME PARK AND ADJACENT FIELDS

These variations are also apparent in the FM arrays printed in Fig. 2.
Note the variation in FM values between pixels with corresponding range
bin and line coordinates. It has been discovered that the information con-
tent in these variations is significant in feature discrimination as is
demonstrated in the final sections of this paper.

4.0 SAMPLE VARIANTS

Four variants were generated from the 4-look FM data discussed previously.
The four sequential values representing each pixel, converted to power units,
were used to generate four variants employed in the classification model.
The FM values are related to power by $M=8 \log_2 P$ plus a constant so the
conversion to power from the log filter magnitudes is given by

$$P = K(2^{M/8}) \quad , \tag{1}$$

where K is a calibration factor which may change from scan to scan or within
a single scan. To illustrate the classification model, data were selected
from regions within the scan over which K remained constant.

The four target variants based on measurement are the mean, Z_1; sample
variance, Z_2; fast variation, Z_3; and slow variation, Z_4, defined as

$$Z_1 = \frac{1}{4} \sum_i P_i \tag{2}$$

$$Z_2^2 = \frac{1}{3} \sum (P_i - Z_1)^2 \tag{3}$$

$$Z_3 = [|P_1 - P_2| + |P_2 - P_3| + |P_3 - P_4|]/3 \tag{4}$$

$$Z_4 = [|P_1 - P_3| + |P_2 - P_4| + |P_1 - P_4|]/3 \tag{5}$$

It should be noted in the above relations that variants 1 and 2 do not
involve time sequence of the data whereas the variants, fast variation and
slow variation, do involve the time sequence of the returns. Other measures
of dispersion investigated, but not reported here include average deviation,
color, deviation from color, total variation, spread, and slope.

5.0 STATISTICS OF THE VARIANTS

5.1 DISTRIBUTIONS INVESTIGATED FOR THE VARIANTS

Since the probability distribution function of the measured data or variants
derived from the measured data was required in the formulation of the classi-
fication model, histograms of the distributions of the various variants were
constructed from the sample data sets. Four standard probability distri-
bution functions, which included the Lognormal, the Weibull, the Chi-Square,
and the Rayleigh PDF's, were fitted to the data. It was found that the Log-
normal and Weibull PDF's generally fitted the test data well with the Weibull
PDF giving a better fit than the Lognormal PDF.

The Lognormal and the Weibull distributions are written as

$$p(X) = \frac{1}{\sqrt{2\pi}X\sigma_{LN}} \exp\left\{-(\ln(X/M))^2/2\sigma_{LN}^2\right\} \tag{6}$$

and

$$p(X) = \frac{n}{\sigma_W} (X/\sigma_W)^{n-1}\exp\left\{-(X/\sigma_W)^n\right\} \tag{7}$$

respectively, where M is the median of X, σ_{LN} is the standard deviation of
$\ln(X/M)$, σ_W is a scale factor, and n is a shape parameter.

5.2 EXAMPLE HISTOGRAMS AND CURVE FITS

Histograms of unnormalized power for samples of rough grass and mobile homes
along with the corresponding Lognormal curve fits are shown in Fig. 7 for
returns from individual SAR maps for each of the four looks with 1:1 overlay.
It should be noted that there is little change in the distribution curves
between maps for the two extremes of power levels represented by the two
classes. The distribution and curve fits, both Lognormal and Weibull, are
also shown in the same figure. The Lognormal, in general, appears to fit the
histogram data but, for some data, does not appear to be well centered about
the histogram data. This apparent anomaly occurs whenever σ_{LN} is large (on
the order of 1.50). Histograms and Lognormal distributions for received
power for the four target types are shown in Fig. 8. These curves show that
the Lognormal distribution is a good representation for the PDF for the four
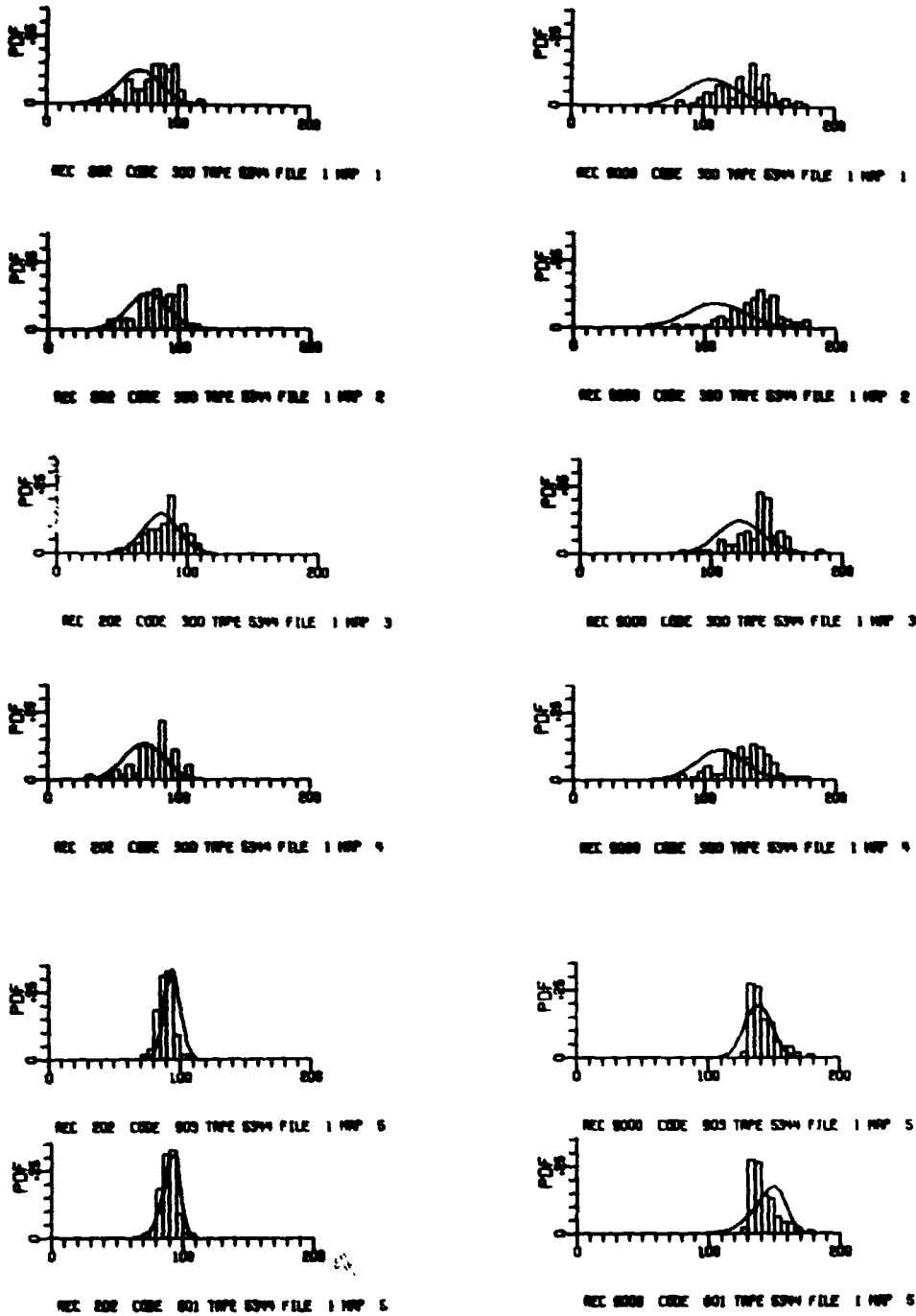sample classes.

FIGURE 7

RECEIVED POWER DISTRIBUTION - HISTOGRAMS AND FITTED LOGNORMAL FUNCTIONS
FOR TWO TARGET TYPES SHOWING TYPICAL VARIATION BETWEEN MAPS. THE LOWER
SET WHICH SHOWS THE 4-MAP MEANS ALSO SHOWS A COMPARISON BETWEEN THE WEIBULL
AND LOGNORMAL PDF.

FIGURE 8

SINGLE MAP RETURN POWER DISTRIBUTIONS FOR FOUR CLASSES OF TARGETS
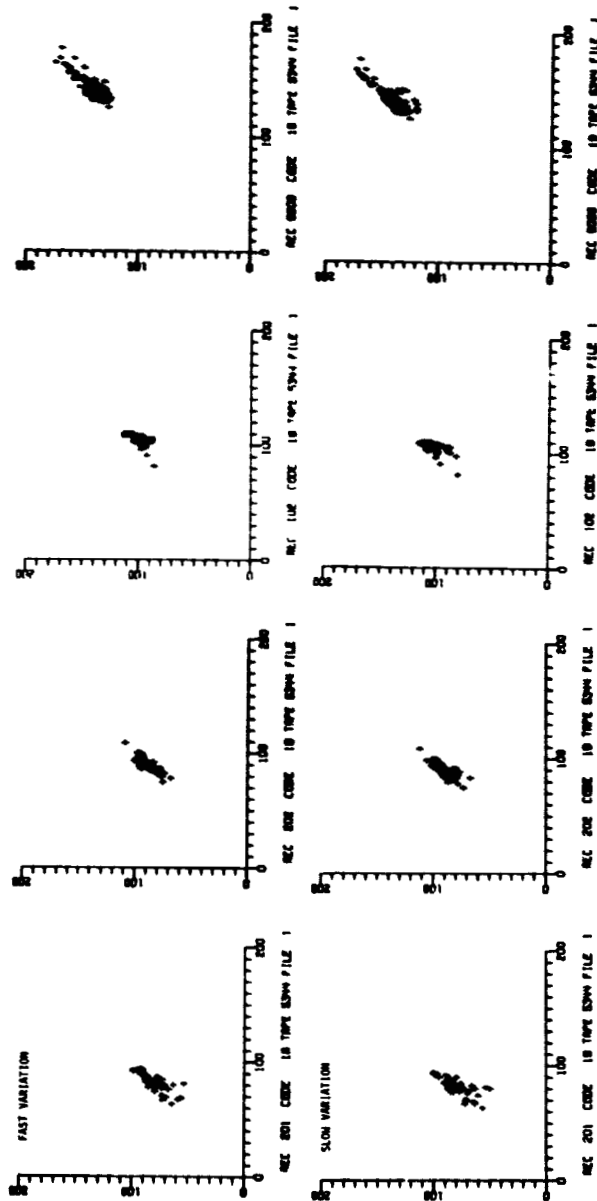
FIGURE 9

SCATTERGRAMS OF FAST VARIATION IN POWER VERSUS MEAN POWER AND OF SLOW
VARIATION IN POWER VERSUS MEAN POWER FOR FOUR CLASSES OF TARGETS

To further illustrate the dispersion of the variants between sample classes,
a sample set of crossplots of the variants, fast and slow variation, versus
mean power is shown in Fig. 9 for the four classes..

6.0 A MULTIVARIANT DISCRIMINANT MODEL AND RESULTS WHEN APPLIED TO A TEST CASE

6.1 CHOICE OF THE CLASSIFICATION MODEL

To demonstrate the utility of several of the variants currently being studied
for discrimination, a classification model based on the statistics of selected
variants derived from the SAR return data was formulated and applied to the
test sample. Four variants and four classes of objects were used to demon-
strate the effectiveness of the Discriminant Model; however, it should be
noted here that the model is by no means limited to these dimensions.

Although the Weibull PDF (Probability Distribution Function) fitted the
variants for all four classes comprising the test sample, the Shape Factors
were large numbers for some targets, thereby making the Weibull PDF less
suitable than the Lognormal PDF for construction of the classification model.
Consequently, the Lognormal distribution was chosen for constructing the
classification model.

6.2 DESCRIPTION OF THE MODEL

The variants, (Z_1, Z_2, Z_3, Z_4), derived from on... ...t of measurements are
assumed to belong to one of four sample classes comprising the test sam-
ple. Since these quantities have a Lognormal distribution, the PDF of Z,
when Z belongs to class T_i, is represented by $p(Z|T_i)$ and for the vector Z is
given by the following:

$$p(Z|T_i) = \frac{1}{(2\pi)^2 |C_i|^{1/2} Z_{pi}} \exp\left\{-\frac{1}{2}(Z' \, C_i^{-1} \, Z)\right\} \qquad (8)$$

where

$$Z = [\ln(Z_1/M_{i1}) \quad , \quad \ln(Z_2/M_{i2}) \quad , \quad \ldots \quad \ln(Z_4/M_{i4})]$$

Z' is the transpose of Z, and

$$Z_{pi} = \prod (Z_r/M_{ir})$$

M_{ir}, for $r=1,2,3,4$, are the medians of Z_r when Z_r belongs to T_i. C_i is the covariance matrix of Z. A decision function is formed that assigns each vector Z to one of the sample classes. This function will assign Z to class T_i if the following condition

$$p(Z|T_i) > p(Z|T_j) \qquad (9)$$

is met for all j not including i.

Inserting the expression

$$r_{ij} = \ell n \frac{p(Z|T_i)}{p(Z|T_j)} \qquad (10)$$

into the ratio of two probability density functions, one obtains a decision function as follows

$$r_{ij} = -\frac{1}{2}\left[\left(\ell n \frac{Z_i}{M_i}\right)' C_i^{-1}\left(\ell n \frac{Z_i}{M_i}\right) - \left(\ell n \frac{Z_j}{M_j}\right)' C_j^{-1}\left(\ell n \frac{Z_j}{M_j}\right)\right]$$

$$+ \frac{1}{2}\ell n \frac{C_j}{C_i} + \sum_r \ell n \left(\frac{M_{jr}}{M_{ir}}\right) \qquad (11)$$

A decision is now made, based on Eq. (11), as to which class Z belongs. By Eq. (9), Z is assigned to Class T_i if $r_{ij}>0$, and is not assigned to T_i if $r_{ij}<0$.

For the selected example given here, only the diagonal terms in the covariance matrices were retained. The off-diagonal terms were set to zero. All combinations for r_{ij} were computed and Z was placed in class k when the condition $r_{kj}>0$ was met for all j.

6.3 TEST RESULTS

Employing the data representing the four sample classes described in section 4, the model was tested against each data point for several combinations of measurement vectors Z. The result of one test is shown in Table I when the four variants--Mean$_{pwr}$, Standard Deviation$_{pwr}$, Fast Variation, and Slow Variation--were employed in the model. As is shown in Table I, data points of class 102 (young fruit trees in an orchard) were identified

TABLE I

NUMBER OF CORRECT AND INCORRECT CLASSIFICATIONS
FOR EACH PIXEL VERSUS EACH CLASS

Class	Class Description	Number of Samples	Number of Classifications per Class			
			102	201	202	9000
102	Fruit Trees	50	34	5	11	0
201	Mowed Grass Field	49	0	44	5	0
202	Unmowed Grass & Weed Field	54	1	40	14	0
9000	Metal Mobile Homes	37	0	0	0	37

correctly by a ratio of slightly better than 2:1 over incorrect classifications as belonging to the grass classes 201 and 202. The ratio of correct to incorrect classifications for the mowed grass class (201) was nearly 9:1 and here the incorrectly classified pixels were classified as belonging to the rough grass class. The ratio of correct to incorrect for the rough grass pixels (202) was about 1:4, a poor showing. However, the grasses were initially selected to test the variants for two very similar subclasses. Considering this fact, the model did surprisingly well. All class 9000 (metal structures) were correctly classified, a 100% performance.

6.4 CONCLUSIONS

Since the results presented here are preliminary , no optimization or detailed analysis of the model or variants has been accomplished . However , it is believed that the evidence presented in this paper indicates that map to map scintillations for the type SAR studied do contain potentially valuable object and feature classifier information .

7.0 ACKNOWLEDGEMENTS

8.0 REFERENCES

1. G. Hahn and S. S. Shapiro, Statistical Models in Engineering, John Wiley and Sons, 1967.

2. W. J. Szajnowski, Estimators of Log-Normal Distribution Parameters, IEEE Trans. on Aerospace and Electronics Systems, Vol. AES-13, No. 5, September 1977.

3. W. J. Szajnowski, Discrimination Between Log-Normal and Weibull Clutter, IEEE Trans. on Aerospace and Electronics Systems, Vol. AES-13, No. 5, September 1977.

4. Julius T. Tou and R. G. Gonzales, Pattern Recognition Principles, Addison-Wesley Publishing Co., 1974.